"Keeping on Track": Firing of Hippocampal Neurons during Delayed-Nonmatch-to-Sample Performance

Robert E. Hampson, John D. Simeral, and Sam A. Deadwyler

Department of Physiology and Pharmacology and the Neuroscience Program, Wake Forest University School of Medicine, Winston-Salem, North Carolina 27157

Hippocampal neurons that encode critical events during a delayed-nonmatch-to-sample (DNMS) task were proposed to have functional topography as demonstrated by Hampson et al. (1999b). Functional cell types (FCTs) that encode similar task features were located within alternating transverse segments along the hippocampal longitudinal axis. On this basis, Redish et al. (2001) suggested that firing of populations of CA1 neurons recorded from the same hippocampal locations in animals running on linear or curvilinear tracks should be spatially and temporally correlated; however, they failed to find such correlations. The current study addresses the issues raised by Redish et al. (2001). Initially we found that modeling of simulated place fields revealed absences in temporal correlations in the study by Redish et al. (2001) that should have been present given the reported spatial correlations. In addition, the correlation methods used by those investigators failed to detect robust but transient event-related cross-correlations between FCTs in the DNMS task. Furthermore, demonstration of such transient, short-latency correlated firing between similar CA3 and CA1 FCTs corroborated the anatomic scheme proposed by Hampson et al. (1999b) and reaffirmed the potential existence of a functional topography within hippocampus.

Key words: ensemble; learning; memory; behavior; place field; cross-correlation

Theories of the function of the hippocampus range from strictly mapping the environment (O'Keefe and Nadel, 1978) to representing relationships between stimuli (Cohen and Eichenbaum, 1993). Paradoxically, because the hippocampus is assumed to encode places, routes, and destinations, it might be expected that a topography of place representation would emerge, but this type of topography has not been identified. However, a previous report by Hampson et al. (1999b) showed that neurons that encoded task-relevant features of a delayed-nonmatch-to-sample (DNMS) task were distributed or "clustered" within defined segments of hippocampus, providing supportive evidence of a functional topography (Eichenbaum et al., 1989).

Recently, Redish et al. (2001) contested this finding, showing that ensembles of hippocampal CA1 neurons recorded in animals traversing elevated linear and curvilinear tracks failed to exhibit clustering of spatial or temporal characteristics. Their results countermand the notion of a functional topography, suggesting that the role of the hippocampus as stated is to "make arbitrary associations," the capacity for which would be compromised if synaptic inputs to adjacent or localized groups of pyramidal cells were correlated (Redish et al., 2001).

In the following report we address these issues directly by (1) exploring whether temporal clustering between cells with overlapping place fields could be detected within data modeled from Redish et al. (2001); and (2) examining the sensitivity of the cross-correlation technique to the temporal domain across which the correlation is calculated (i.e., entire spike train vs perievent epochs). New evidence for temporal correlations between clusters of functionally identified hippocampal neurons is also introduced that validates the findings of Hampson et al. (1999b).

MATERIALS AND METHODS

Simulation of place fields on linear tracks. Monte Carlo methods were applied to simulate track-running experiments using place-cell parameters derived from previous published reports (Skaggs and McNaughton, 1996; Skaggs et al., 1996; Redish et al., 2000, 2001). The parameters used in the simulations were: track length, 180 cm; traversal speed, 15 cm/sec; pixel size, 2.8 cm; place field width, 50 cm (all pixels with above background firing rate); mean simultaneously recorded neurons, 22; and recording time, 30 min. Fields were randomly distributed assuming bidirectional traversal (360 cm) to allow for neurons that fired only in one direction (Skaggs et al., 1996). Each spike train comprised 40 laps over the track (20–30 sec each). Place fields were simulated with a Gaussian function (Mehta et al., 2000) centered on a single point on the track with increased firing from background (0.5–2.0 Hz) to 15–20 Hz at the peak. Each cell was assumed to fire in its place field on every lap. Spatial cross-correlation coefficients (ρ) between pairs of simulated place fields were computed from spike trains sorted into 128 bins (64 pixels for each outbound and inbound lap), normalized for time spent in each pixel. Temporal cross-correlations were computed as per Redish et al. (2001)

Received July 27, 2001; revised Sept. 10, 2001; accepted Sept. 17, 2001.

This work was supported by National Institutes of Health (NIH) Grants DA08549 and MH61397 to R.E.H. and DA03502 and DA00119 to S.A.D. All animal procedures followed NIH and Society for Neuroscience guidelines for care and use of laboratory animals.

Correspondence should be addressed to Dr. Robert E. Hampson, Department of Physiology and Pharmacology, Wake Forest University School of Medicine, Medical Center Boulevard, Winston-Salem, NC 27157-1083. E-mail: rhampson@wfubmc.edu.

This article is published in *The Journal of Neuroscience*, Rapid Communications Section, which publishes brief, peer-reviewed papers online, not in print. Rapid Communications are posted online approximately one month earlier than they would appear if printed. They are listed in the Table of Contents of the next open issue of JNeurosci. Cite this article as: JNeurosci, 2002, 22:RC198 (1–6). The publication date is the date of posting online at www.jneurosci.org.

http://www.jneurosci.org/cgi/content/full/5983

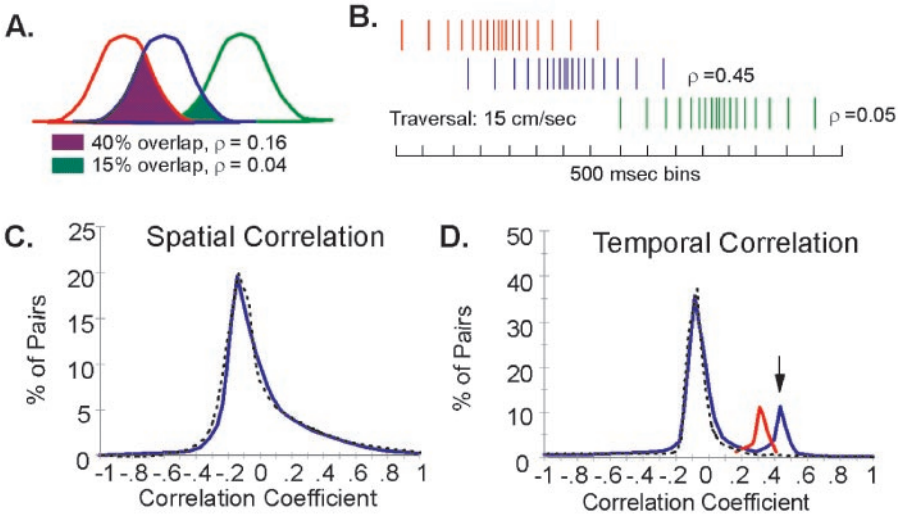

Figure 1. Monte Carlo simulation of place fields recorded while animals traversed a linear track, derived from parameters reported by Redish et al. (2000, 2001). The simulation included 3000 neurons, comprising 128 ensembles and 53,936 correlated pairs (see Materials and Methods for parameters). *A*, Place-field firing was modeled with Gaussian function as illustrated. Nearest neighbor fields (*red*/*blue*) produced a mean 40% overlap (*purple regions*) and nonadjacent fields (*red*/*green*) produced <15% overlap (*green regions*); ρ indicates spatial cross-correlation. *B*, Temporal dispersion (rasters) of cell firing in *A*. Neural spike trains (*colored ticks*) were binned in 500 msec increments (30 min total); ρ is temporal cross-correlation. Overlapping fields (*red*/*blue*) were separated by 1.09 sec and nonoverlapping fields (*red*/*green*) were separated by >3.5 sec. *C*, Distribution of spatial cross-correlation coefficients (*blue line*) from simulation. The *dotted line* indicates correlations reported by Redish et al. (2001). Peak at $\rho = -0.10$ reflects 80% of pairs with nonoverlapping place fields. Asymmetry biased toward positive correlations reflects ~20% of pairs with overlapping place fields. *D*, Temporal cross-correlation coefficient distribution (*blue line*). The main peak ($\rho = -0.10$) reflects nonoverlapping fields; the secondary peak ($\rho = 0.46$, *arrow*) indicates 10% of cell pairs with >40% overlapping place fields (i.e., nearest neighbors). The *dotted line* indicates the distribution published by Redish et al. (2001). Reduction in field size (25 cm) or traversal speed (10 cm/sec) shifted the secondary peak to the left (*red trace*) without decreasing amplitude.

from spike-train firing by dividing cell firing into 500 msec bins and computing the Pearson cross-correlation coefficients (ρ) across the entire spike train. Statistical tests on the distributions of coefficients used the Komolgorov–Smirnov *D* statistic for $n > 2000$ and the Anderson–Darling A^2 statistic (D'Agostino and Stephens, 1986) for $n < 2000$ (i.e., comparison between same vs different tetrode).

Recording techniques. Male Long–Evans rats ($n = 27$, 3–11 months of age) were trained to criterion on a two-lever spatial DNMS task with randomly occurring delays of 1–40 sec. Recording arrays (NB Laboratories, Denison, TX) with 16 microwires (40 μm) were surgically implanted and positioned within the CA1 and CA3 cell layers (Deadwyler et al., 1996). Arrays consisted of eight wire pairs with 200 μm separation between pairs and 800 μm wires within a pair. Electrode tip length was precisely trimmed to follow the longitudinal curvature of the hippocampus (Deadwyler et al., 1996). Recordings were obtained from 312 pyramidal neurons (9–16 per animal; mean = 11.5) as determined by firing rate criteria (Fox and Ranck, 1981). Stable extracellular action potential waveforms from at least five DNMS sessions were monitored, and consistent event-specific firing patterns were assessed by constructing normalized perievent histograms of firing rate ± 1.5 sec around each task-relevant event or leverpress. Only the largest amplitude waveform (neuron) per electrode position was used to guarantee the best estimation of relative location in the hippocampus. Perievent firing frequency relative to baseline was transformed to a *z* score to determine encoding as significantly elevated firing ($z \geq 3.09$; $p < 0.001$). Each neuron was identified with respect to its functional cell type (FCT) depending on which DNMS event(s) it encoded (e.g., a unique event, left nonmatch response; or category, all left leverpresses). Cells with background firing rates of >2.0 Hz were excluded from analysis to avoid contamination by interneuron activity. Temporal cross-correlation coefficients (ρ) were calculated across entire neural spike trains as described above. Cross-correlograms were constructed from normalized spike-triggered histograms computed at 1.0 msec resolution during designated time epochs. Coefficients (ρ) reported for correlograms differed from those calculated over complete spikes trains in that (1) they only included spikes during the designated time epoch, (2) bins were 1 msec, and (3) bins were adjusted for latency of the correlogram peak.

RESULTS

Assessment of hippocampal cell firing on linear tracks

Reported firing contingencies of hippocampal place cells assessed on linear tracks indicate that discrete spatial segments are mapped as the animal runs in a single direction along the track (Skaggs and McNaughton, 1996; Redish et al., 2000). Using this procedure, Redish et al. (2001) failed to observe significant spatial or temporal correlations between cells or fields on the same versus different tetrodes arranged in a lattice of 14 with a minimum 350 μm separation. We explored the firing correlates in those studies by simulating 3000 place fields recorded on linear tracks using the descriptions of place field and track parameters published by Redish et al. (2000).

Ensembles of 8–46 simultaneously recorded place cells (Redish et al., 2000) were simulated assuming random distribution of place fields within an ensemble. In that context, if seven or more 50-cm-wide place fields were recorded, at least one field would overlap another, whereas with >20 fields recorded, each field would have a mean of 40% overlap with the two "nearest neighbors" (Fig. 1*A*). Furthermore, an "average" ensemble containing 22 neurons (Redish et al., 2000) would have 21 possible cross-correlation pairings for each place field: 19 (90.5%) with low spatial correlation ($\rho < 0.05$, no overlap) because of extended separation distance on the track (Fig. 1*A*). However, ~10% of place-field pairs (2 of 21, 9.5%) would overlap as nearest neighbors and possess stronger spatial correlations ($\rho \geq 0.2$).

The results of the simulation are shown in Figure 1*C*. The distribution of spatial correlation coefficients (Fig. 1*C*, *blue trace*) for the simulation was identical to the graph (Fig. 1*C*, *dotted trace*) shown by Redish et al. (2001, their Fig. 3*a*). Temporal correlations between pairs of spike trains (Fig. 1*B*) were stronger (mean of $\rho = 0.46$) in the 10% of cell pairs with overlapping fields (Fig. 1*D*, *blue trace*, *arrow*) compared with the 90% of cell pairs with fields that did not overlap ($\rho \leq 0.05$). Interestingly, Figure 3*b* of Redish et al. (2001) does not show this secondary peak (Fig. 1*D*, *dotted trace*) or any indication of increased correlations produced by overlapping fields. Considering that they reported spatial correlations identical to the simulation (Fig. 1*C*, *dotted trace*), the absence of this secondary peak for overlapping fields is puzzling.

Additional investigation of the strong correlations in Figure 1*C* revealed that field overlap must be reduced to ≤15% to eliminate the secondary peak. Decreasing place field size by one-half produced the same percentage of overlapping fields with only slightly reduced correlations ($\rho = 0.33$; Fig. 1*D*, *red trace*). Alternatively, reducing traversal speed to10 cm/sec also reduced the magnitude

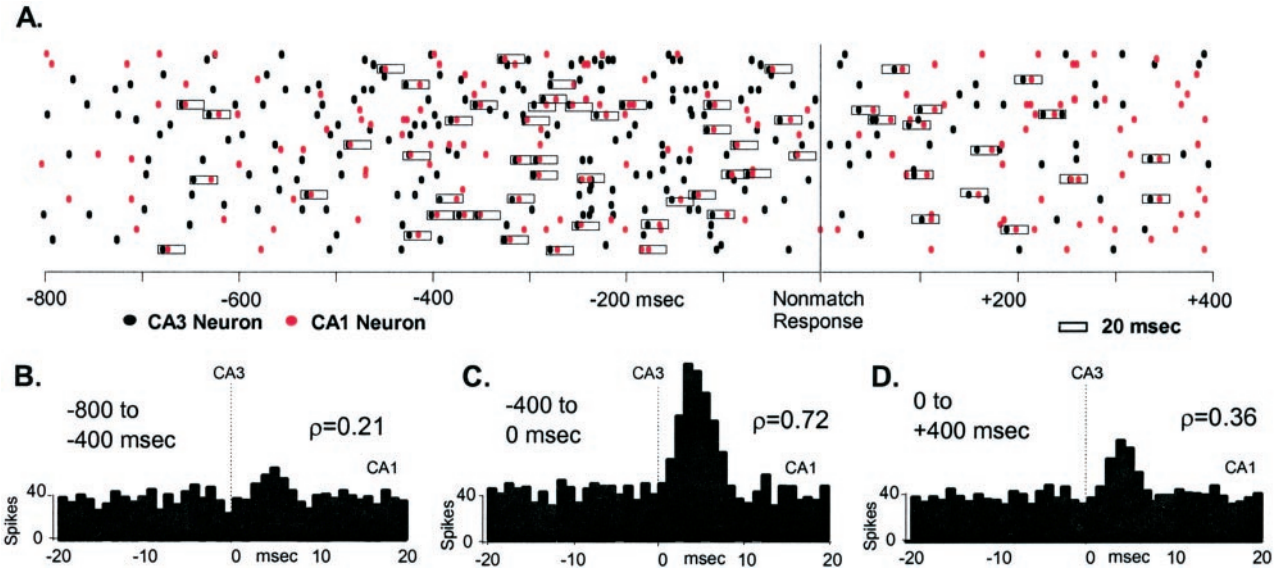

Figure 2. Transient cross-correlations between simultaneously recorded FCTs encoding the same DNMS behavioral event. *A*, Rastergrams of single trial firing. *Black dots*, CA3 FCT; *red dots*, CA1 FCT. Each row is a single trial, 800 msec before to 400 msec after nonmatch response (0 msec). *Rectangles* indicate when both neurons fired within 20 msec; increased rectangle frequency reflects a significant increase ($X^2_{(8)} = 32.41$; $p < 0.001$) in correlated firing. *Bottom panels*, Cross-correlograms of CA3 spike-triggered CA1 firing, constructed over 100 trials within each of the three indicated time epochs: *B*, −800 to −400 msec; *C*, −400–0 msec; *D*, 0 to +400 msec. Coefficients (ρ) indicate correlation measured at peak of normalized correlogram. Mean across complete trial, $\rho = 0.08$.

of correlation ($\rho = 0.36$) but not the percentage of correlated pairs. Only a significant reduction in both field width (15 cm) and speed (5 cm/sec) eliminated the second peak in Figure 1*D* (Komolgorov–Smirnov *D* statistic = 0.59; $K_{sa} = 0.68$; $p > 0.25$). Two other factors were also examined: the Gaussian nature of place-field firing (Mehta et al., 2000) and consistency on each pass through the field (Fenton and Muller, 1998). Reduced secondary peaks ($\rho < 0.20$) were produced only if one of the neurons in a pair failed to fire on 80% of passes through the field, or if random firing in the field occurred. From the above "unrealistic conditions" required to eliminate the secondary peak of temporal correlations in the model given the distribution of spatial correlations (Fig. 1*C*), it appears that there were inconsistencies in the data reported by Redish et al. (2001).

Finally, cells recorded from the same tetrodes were examined as to whether they showed stronger spatial or temporal correlations (clustering) than cells on different tetrodes (Redish et al., 2001). Simulated place cells were separated into different tetrode sets and analyzed. When neurons recorded from the same tetrode (within) were clustered, the secondary peak (Fig. 1*D*, *arrow*) of strong temporal correlations between nearest neighbor place fields was increased from 9.5 to 31% ($A^2 = 0.87$; $p < 0.05$), compared with a decrease from 9.5 to 5.6% for between-tetrode pairs. Thus, to resolve the issue, it is necessary for a secondary population of strong correlations to be present for overlapping fields, to identify clustering if it exists. Because this peak was not present in the data obtained by Redish et al. (2001), it would have been impossible to detect clustering if it were present.

Transient versus continuous spike train correlations

Redish et al. (2001) computed cross-correlation coefficients across complete spike trains for the entire sessions. We constructed cross-correlations between FCTs (see Materials and Methods) that were either (1) confined to temporal epochs surrounding the appropriate behavioral events or (2) computed across the entire trial. Figure 2 shows superimposed rastergrams and cross-correlograms from two different FCTs analyzed in relation to their behavioral correlate (nonmatch response). The small rectangular boxes (Fig. 2*A*) capture instances in which one neuron discharged within 20 msec of the other. It is clear that both cells increased firing just before the response (−400–0 msec) and also exhibited a transient increase in the number of correlated or "captured" spikes (spike-triggered cross-correlogram, Fig. 2*C*). However, correlated firing was minimal in the −800 to −400 msec epoch (before the response) and the 0 to +400 msec epoch (Fig. 2*B,D*). Thus calculation of the mean correlation coefficient between the spike trains of the same two cells over the entire trial was not significant ($\rho = 0.08$). Coefficients calculated indiscriminately across the entire spike train tend to dissolve the robust transient temporal correlations between FCTs during task-relevant events (Fig. 2).

FCTs and interneurons fire differently during DNMS trials

Recently, Hirase et al. (2001) showed that local coherence could occur in hippocampal pyramidal cell firing as a result of shifts from theta (wheel running) to nontheta (sleep or immobility) behavioral states. They also suggested that these states coexist during certain behavioral contexts and could provide the basis for reciprocal firing between interneurons and FCTs during the DNMS task. Coherent firing during nontheta states could thus account for the apparent clustering of FCTs within defined hippocampal regions (Hampson et al., 1999b). We investigated this by examining simultaneous interneuron and FCT firing during the DNMS task. The panels in Figure 3 show activity of three different interneurons (Fig. 3, *top*) with associated FCTs (Fig. 3, *bottom*). The autocorrelations show that the three interneurons had intrinsic 80–160 msec periodicity indicative of "theta" cell firing (Csicsvari et al., 1998). The increased FCT firing relative to their appropriate events was not associated with a marked change

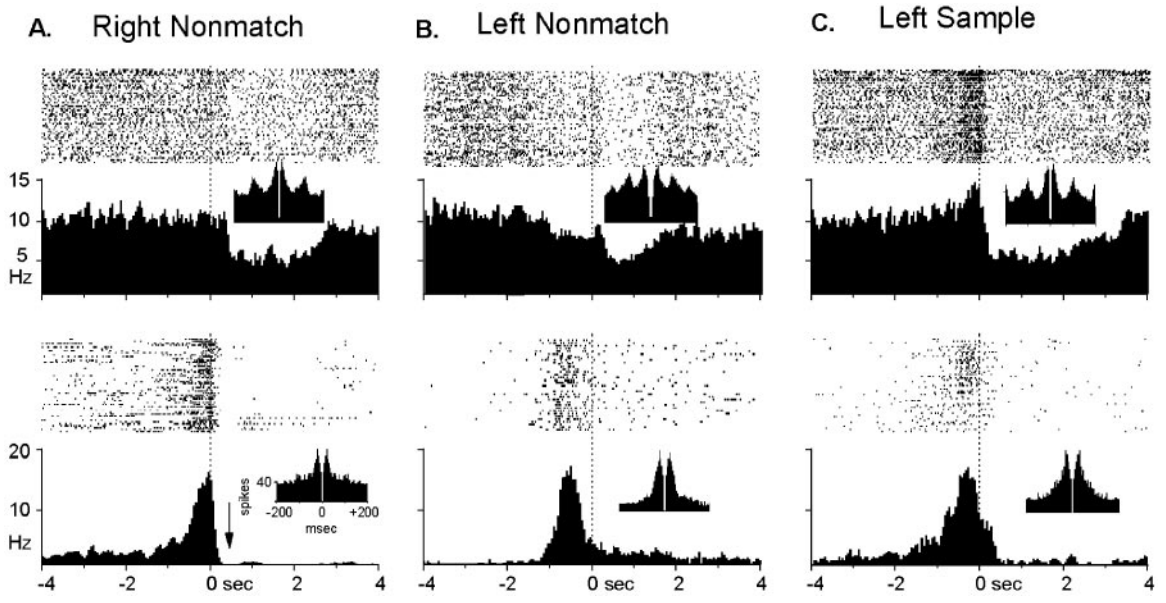

Figure 3. Comparison of interneurons and FCTs. *Top*, Rastergrams and perievent histograms for three different interneurons. *Bottom*, Rastergrams and perievent histograms for three simultaneously recorded FCTs. *A*, Interneuron and FCT firing recorded during (±4 sec) right nonmatch response. *Arrow*, Interneuron firing decreased 50% from baseline during drinking. The periodicity of the interneuron autocorrelogram (*inset*) was 120 msec (8 Hz). *B*, A different interneuron–FCT pair recorded during left nonmatch response. The periodicity of interneuron was 90 msec (11 Hz). *C*, A third interneuron–FCT pair recorded during left sample response. The interneuron firing rate decreases during delay. The periodicity of the interneuron was 100 msec (10 Hz). *Insets*, Autocorrelograms ±200 msec; the refractory period at the *center* is 2 msec.

in interneuron firing in either of the three cell pairs (Fig. 3, *top*). Alternatively, the substantial decrease in firing of each of the three interneurons after completion of the response was also not associated with a reciprocal increase in FCT discharge (Fig. 3*A*, *arrow*).

Hippocampal FCTs are clustered and correlated

Hampson et al. (1999b) defined clusters on the basis of groups of FCTs recorded with linear multielectrode arrays, within interleaved transverse zones or sectors along the septotemporal axis of the hippocampus. To test the stipulation by Redish et al. (2001) regarding clustering (cited in the introductory remarks), we constructed cross-correlograms between FCTs within their appropriate epochs, as shown in Figure 2. The regions designated right sector and left sector in the foldout map of the hippocampus in Figure 4 correspond to locations of FCTs that encoded right and left leverpresses in the task. Figure 4 shows correlograms and mean peak correlations for respective identical (encoded same event, $n = 24$), compatible (encoded at least one event feature; e.g., left or sample, $n = 56$) and incompatible (encoded no common features, $n = 296$) pairs of CA3 and CA1 FCTs sorted by electrode position on the array. The correlograms on the right correspond to comparisons (Fig. 4, *solid arrows*) between identical FCTs in the left sector (Fig. 4, *triangles*). In all three cases, correlated firing of CA1 FCTs was significant (0 μm, $\rho = 0.31 \pm 0.07$; 200 μm, $\rho = 0.71 \pm 0.11$; 400 μm, $\rho = 0.49 \pm 0.09$; $X^2_{(80)} = 379.2$; $p < 0.001$), with the strongest correlation between pairs at 200 μm of septotemporal offset, CA1 relative to CA3. An important finding in this regard was that two identical CA1 FCTs, both with strong correlations to the same CA3 FCT, showed strong correlations with each other (Fig. 4, *CA1–CA1*; $\rho = 0.058 \pm 0.19$) at negligible peak latencies (1.25 ± 0.39 msec), indicating potential coactivation by that same CA3 neuron (Hirase et al., 2001).

The top left correlogram in Figure 4 shows the expected nonsignificant correlation ($\rho = 0.06 \pm 0.05$) between incompatible FCTs (Fig. 4, *dotted arrow*) located in different hippocampal sectors. Below that appear highly significant correlations between identical FCTs (Fig. 4, *stars*) located in the opposite (right) sector. Finally, correlations between compatible FCTs, illustrated in the center bottom panel (Fig. 4, *circles*), were significant ($\rho = 0.33 \pm 0.10$), but less so than between identical FCTs.

DISCUSSION

In the above analysis, we have demonstrated that the failure of Redish et al. (2001) to find the clustering reported by Hampson et al. (1999b) requires serious reconsideration on the basis of (1) an inability to demonstrate significant correlated firing in place cells given the spatial overlap parameters they reported, (2) their use of cross-correlation techniques that could not resolve robust but transient correlated cell firing, and (3) additional evidence provided here demonstrating short-latency correlated firing between FCTs in accordance with the topographic scheme proposed by Hampson et al. (1999b).

Redish et al. (2001) found no clustering in animals running on linear tracks; however, evidence for clustering by their definition could occur in only 10% of the cell pairs tested (i.e., those with fields that overlapped on the track). Their report did not reflect the necessary percentage of strong temporal correlations dictated by their distribution of spatial correlations, despite previous demonstrations of strong correlations as a necessary consequence of place-field overlap (Wilson and McNaughton 1994; Skaggs and McNaughton 1996; Skaggs et al., 1996). Differential clustering either between or within tetrodes in the model did not account for this absence (Fig. 1*D*). Given their method of correlation across continuous spike trains on linear tracks, detection of clustering is difficult because the majority of coefficients are negligible or zero because of the large number of non-overlapping fields.

The definition of clustering proposed by Redish et al. (2001) stated that neurons recorded from the same location should be

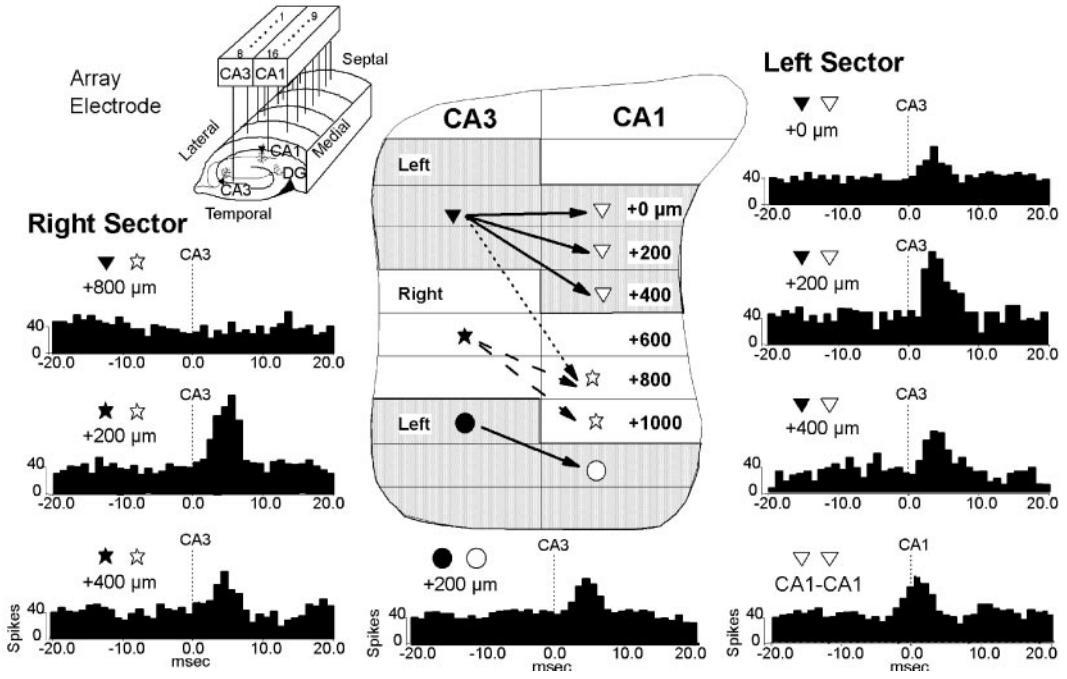

Figure 4. Anatomic distribution of cross-correlations. The hippocampal foldout map shows pairs of FCTs classified as identical (*triangles*, *stars*), compatible (*circles*), or incompatible (*different symbols*) located in registered electrode array positions (*inset*). Left (*shaded*) and right (*unshaded*) sectors (600 μm) refer to encoding of left versus right leverpresses in DNMS. *Left sector*, Correlograms from three pairs of identical CA3–CA1 FCTs (*triangles*, *solid arrows*), measured within $\pm$1.5 sec epochs surrounding task events, summed over 100 trials. *Bottom panel*, Correlogram for pair of CA1–CA1 FCTs (0 and 200 μm) correlated with the same CA3 FCT (*filled triangle*) and each other (note: 0 msec peak latency). *Right sector*, Correlogram (*top*) constructed between incompatible (i.e., different sectors) CA3–CA1 FCTs (*dotted arrow*). *Bottom panel*, Correlograms for two pairs of identical FCTs (*stars*, *dashed arrows*). *Center bottom panel*, Correlogram for pair of compatible (sample and left) FCTs during a commonly encoded left sample event.

both spatially and temporally correlated. Given this interpretation, we showed that transient correlations between FCTs were robust and differential depending on their anatomic location in the hippocampus (Fig. 4); however, these correlations were eliminated if calculated indiscriminately across the entire trial (Fig. 2). The 200 μm offset in the gradient of strongest correlations ($p = 0.71$; $p < 0.001$) between CA3 and CA1 FCTs in the same animals (Fig. 4) is supported by the original description of "lamellas" by Andersen et al. (1969). This description was reassessed recently (Andersen et al., 2000) to show that the densities of functional synaptic projections from CA3 to CA1 form a diagonal "ridge" between the two subregions that is most dense at the 200 μm offset between the two regions. Such evidence strongly supports the functional topography proposed by Hampson et al. (1999b).

Redish et al. (2001) also suggested that the two behavioral contexts, running on linear tracks and DNMS performance, are fundamentally the same with respect to hippocampal correlates. This assumption can be questioned from several perspectives. We have in the past shown the necessity of hippocampal cell firing in the DNMS task by demonstrating that (1) successful performance requires an intact hippocampus as well as several weeks of training (Hampson et al., 1999a), (2) FCTs encode information critical to correct DNMS performance (Hampson and Deadwyler 1996; Deadwyler and Hampson, 1997; Hampson et al., 1998), and (3) DNMS performance is facilitated by drugs that enhance FCT firing (Hampson et al., 1998). In contrast, the hippocampal activity reported by Redish et al. (2001) involved little behavioral plasticity or complexity, and where complexity existed (Redish et al., 2000), the necessity of hippocampal cell firing for accurate performance was not disclosed.

Fox and Ranck (1981) originally reported the differences between theta cell and presumed pyramidal cell firing in awake moving animals. Figure 3 illustrates spontaneous background firing rates (>3 Hz) and oscillations similar to those reported previously for theta cells (Christian and Deadwyler, 1986; Csicsvari et al., 1998; Hampson et al., 1998; Wiebe and Staubli, 2001), which differed markedly from simultaneously recorded pyramidal cells (FCTs). Buzsaki et al. (1983) showed that pyramidal cell firing is released during nontheta (behaviorally immobile) states. This circumstance could explain the increased FCT firing observed in the DNMS task if animals were inactive during the lever press. Figure 3 indicates that FCT firing was not dependent on theta or nontheta states entrained at critical times during the DNMS task, as evidenced by the lack of reciprocity in FCT–interneuron firing either at the time of the response or during reduced locomotion after completion of the response.

A seemingly endless recurring methodological issue relates to the touted differences between tetrode and conventional single electrode recording methods in the hippocampus. We and others have addressed this issue in several previous publications (Nicolelis et al., 1993; Deadwyler et al., 1996; Hampson and Deadwyler, 1998; Chapin et al., 1999). Suffice it to say that ironically, if our recording techniques did reflect multiple and not single FCT activity, it would provide the best possible evidence for clustering. This is because neuronal firing is categorized with respect to when it occurs in the DNMS task. Such multiple FCT firing restricted to specific events would reflect multiple functional cell types with correlated firing active at the same electrode location [i.e., clustering as defined by Redish et al. (2001)].

In summary, the modeled outcomes derived from their data (Fig. 1), the insensitivity of their assessment procedures to strong

transient temporal correlations (Fig. 2), and the demonstration here of temporal correlations between FCTs located in hippocampal sectors defined by the demands of the DNMS task (Fig. 4) mitigate against the negative conclusions of Redish et al. (2001) and provide additional support for the topographic scheme proposed previously by Hampson et al. (1999b). With restricted, precise correlation methods we verified that FCT firing follows an independently determined gradient of functional synaptic connectivity between CA3 and CA1 cells (Andersen et al., 2000) and that such clustering is specific to the cognitive dimensions of the DNMS task. However, it should not necessarily be expected that the clustering observed for one behavioral context (i.e., DNMS) implies a similar relationship in other behavioral contexts (i.e., linear tracks).

REFERENCES

Andersen P, Bliss TV, Lomo T, Olsen LI, Skrede KK (1969) Lamellar organization of hippocampal excitatory pathways. Acta Physiol Scand 76:4A–5A.

Andersen P, Soleng AF, Raastad M (2000) The hippocampal lamella hypothesis revisited. Brain Res 886:165–171.

Buzsaki G, Leung LW, Vanderwolf CH (1983) Cellular bases of hippocampal EEG in the behaving rat. Brain Res 287:139–171.

Chapin JK, Moxon KA, Markowitz RS, Nicolelis MA (1999) Real-time control of a robot arm using simultaneously recorded neurons in the motor cortex. Nat Neurosci 2:664–670.

Christian EP, Deadwyler SA (1986) Behavioral functions and hippocampal cell types: evidence for two nonoverlapping populations in the rat. J Neurophysiol 55:331–348.

Cohen NJ, Eichenbaum H (1993) Memory, amnesia, and the hippocampal system. Cambridge, MA: MIT Press.

Csicsvari J, Hirase H, Czurko A, Buzsaki G (1998) Reliability and state dependence of pyramidal cell-interneuron synapses in the hippocampus: an ensemble approach in the behaving rat. Neuron 21:179–189.

D'Agostino RB, Stephens MA (1986) Goodness-of-fit techniques, pp 97–193. New York: Marcel-Dekker.

Deadwyler SA, Hampson RE (1997) The significance of neural ensemble codes during behavior and cognition. In: Annual review of neuroscience, Vol 20 (Cowan WM, Shooter EM, Stevens CF, Thompson RF, eds), pp 217–244. Palo Alto, CA: Annual Reviews, Inc.

Deadwyler SA, Bunn T, Hampson RE (1996) Hippocampal ensemble activity during spatial delayed-nonmatch-to-sample performance in rats. J Neurosci 16:354–372.

Eichenbaum H, Wiener SI, Shapiro ML, Cohen NJ (1989) The organization of spatial coding in the hippocampus: a study of neural ensemble activity. J Neurosci 9:2764–2775.

Fenton AA, Muller RU (1998) Place cell discharge is extremely variable during individual passes of the rat through the firing field. Proc Natl Acad Sci USA 95:3182–3187.

Fox SE, Ranck Jr JB (1981) Electrophysiological characteristics of hippocampal complex-spike cells and theta cells. Exp Brain Res 41:399–410.

Hampson RE, Deadwyler SA (1996) Ensemble codes involving hippocampal neurons are at risk during delayed performance tests. Proc Natl Acad Sci USA 93:13487–13493.

Hampson RE, Deadwyler SA (1998) Methods, results, and issues related to recording neural ensembles. In: Neuronal ensembles: strategies for recording and decoding (Eichenbaum H, Davis J, eds), pp 207–234. New York: Wiley.

Hampson RE, Rogers G, Lynch G, Deadwyler SA (1998) Facilitative effects of the ampakine CX516 on short-term memory in rats: correlations with hippocampal ensemble activity. J Neurosci 18:2748–2763.

Hampson RE, Jarrard LE, Deadwyler SA (1999a) Effects of ibotenate hippocampal and extrahippocampal destruction on delayed-match and -nonmatch-to-sample behavior in rats. J Neurosci 19:1492–1507.

Hampson RE, Simeral JD, Deadwyler SA (1999b) Distribution of spatial and nonspatial information in dorsal hippocampus. Nature 402:610–614.

Hirase H, Leinekugel X, Csicsvari J, Czurko A, Buzsaki G (2001) Behavior-dependent states of the hippocampal network affect functional clustering of neurons. J Neurosci 21:RC145:1–4.

Mehta MR, Quirk MC, Wilson MA (2000) Experience-dependent asymmetric shape of hippocampal receptive fields. Neuron 25:707–715.

Nicolelis MA, Lin RC, Woodward DJ, Chapin JK (1993) Dynamic and distributed properties of many-neuron ensembles in the ventral posterior medial thalamus of awake rats. Proc Natl Acad Sci USA 90:2212–2216.

O'Keefe JA, Nadel L (1978) The hippocampus as a cognitive map. Oxford: Clarendon Press.

Redish AD, Rosenzweig ES, Bohanick JD, McNaughton BL, Barnes CA (2000) Dynamics of hippocampal ensemble activity realignment: time versus space. J Neurosci 20:9298–9309.

Redish AD, Battaglia FP, Chawla MK, Ekstrom AD, Gerrard JL, Lipa P, Rosenzweig ES, Worley PF, Guzowski JF, McNaughton BL, Barnes CA (2001) Independence of firing correlates of anatomically proximate hippocampal pyramidal cells. J Neurosci 21:RC134:1–6.

Skaggs WE, McNaughton BL (1996) Replay of neuronal firing sequences in rat hippocampus during sleep following spatial exposure. Science 271:1870–1873.

Skaggs WE, McNaughton BL, Wilson MA, Barnes CA (1996) Theta phase precession in hippocampal neuronal populations and the compression of temporal sequences. Hippocampus 6:149–172.

Wiebe SP, Staubli UV (2001) Recognition memory correlates of hippocampal theta cells. J Neurosci 21:3955–3967.

Wilson MA, McNaughton BL (1994) Reactivation of hippocampal ensemble memories during sleep. Science 265:676–679.